Available online at www.sciencedirect.com
ScienceDirect
Bioorganic & Medicinal Chemistry 16 (2008) 2103–2113
Bioorganic & Medicinal Chemistry

Synthesis, adenosine receptor binding and 3D-QSAR of 4-substituted 2-(2′-furyl)-1,2,4-triazolo[1,5-*a*]quinoxalines

Ana Martínez,[a] Hugo Gutiérrez-de-Terán,[b] José Brea,[b] Enrique Raviña,[a,*] Maria Isabel Loza,[b] Maria Isabel Cadavid,[b] Ferran Sanz,[c] Bernat Vidal,[d] Victor Segarra[d] and Eddy Sotelo[a,*]

[a]*Department of Organic Chemistry, Faculty of Pharmacy, University of Santiago de Compostela, Santiago de Compostela E-15782, Spain*
[b]*Department of Pharmacology, Faculty of Pharmacy, University of Santiago de Compostela, Santiago de Compostela E-15782, Spain*
[c]*Unitat de Recerca en Informática Médica (GRIB), IMIM, Dep. CEXS, Universitat Pompeu Fabra, Dr. Aiguader 88, Barcelona E-08003, Spain*
[d]*Medicinal Chemistry Department, Almirall, Treball 2-4, St. Just Desvern, Barcelona E-08960, Spain*

Received 14 June 2007; revised 2 October 2007; accepted 17 October 2007
Available online 24 January 2008

Abstract—A collection of 25 2-(2′-furyl)-1,2,4-triazolo[1,5-*a*]quinoxalines incorporating different substitution patterns at position 4 have been synthesized and their binding affinity towards human adenosine receptors (hA_1, hA_{2A}, hA_{2B} and hA_3) was determinated. The biological data show that several potent at hA_1, but lightly selective, adenosine ligands were identified. Moreover, these results confirmed the hypothesis that the structural modifications carried out on the 4-position of the tricyclic system produces a remarkable modification of the adenosine receptorial profile. A 3D-QSAR modelling study (GRIND/ALMOND methodology) performed on the hA_1 data gave further support to the pharmacological results, and it is presented as a useful tool for the future design of ligands with better pharmacological profiles.

1. Introduction

Interaction of adenosine with a set of specific receptors, classified as A_1, A_{2A}, A_{2B} and A_3, may regulate different physiological functions.[1–5] For this reason, adenosine receptors (AR) are currently considered as attractive targets in the treatment of diverse pathophysiologic disorders,[6–9] particularly, AR antagonists are sought as renal protective,[16–18] anti-Parkinson,[19,20] antiasthmatic,[21,22] antidiabetic,[23] or antiischemic agents.[24,25] AR belong to the superfamily of the G-protein coupled receptors (GPCRs) and therefore they exert their physiological role by activation or inhibition of different second messenger systems.[1] Many efforts have been invested in the search for novel ligands with remarked selectivity,[10–15] either for a given AR subtype or for their tissue distribution. This research not only pursues obtaining potential therapeutic agents, but also useful pharmacological tools. As a result of this, a huge number of AR agonists and antagonists have been synthesized.

The naturally occurring xanthines (e.g., caffeine and theophylline) were the initial prototypic AR antagonists.[26,27] The many attempts to improve their potency and selectivity have resulted in the preparation of a large number of xanthine derivatives, and much is known now in terms of their structure–activity and structure–selectivity relationships, as well as about their pharmacological activity.[28–30] However, most of these xanthine derivatives showed poor water solubility and a high metabolic rate (specially due to their interaction with cytochrome P450 family) which strongly limitate its drugability profile. The extensive research in this topic have also lead to the discovery of different classes of non-xanthine AR antagonists, being most of them nitrogen-containing heterocyclic compounds (Fig. 1).[31–49]

Some of the early described tricyclic adenosine antagonists were identified from collections of compounds

Keywords: Adenosine receptor binding; 1,2,4-Triazolo[1,5-*a*]quinoxalines; 3D-QSAR.
* Corresponding authors. Tel.: +34 981 563100 15221; fax: +34 981 528093; e-mail addresses: qosotelo@usc.es; qofara@usc.es

0968-0896/$ - see front matter © 2008 Elsevier Ltd. All rights reserved.
doi:10.1016/j.bmc.2007.10.103

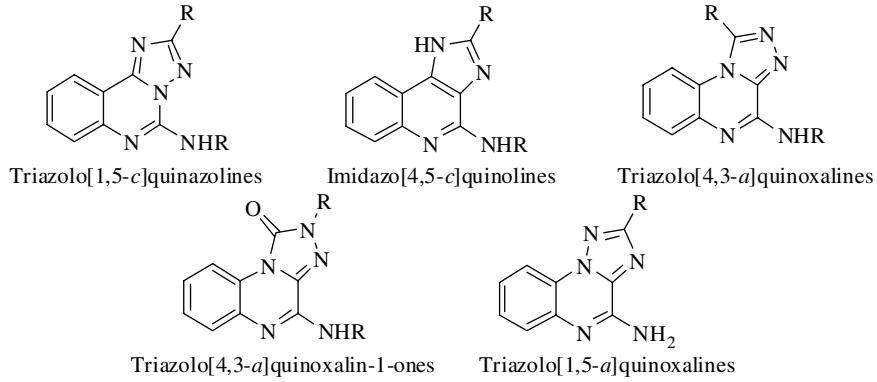

Figure 1. Structure of some representative tricyclic adenosine antagonists.

initially designed as ligands of the benzodiazepine receptors.[35–38] Several elegant examples of the pharmacomodulation of these prototypes have allowed the development of new selective adenosine antagonists.[39–42] Within the huge number of tricyclic heteroaromatic systems tested as adenosine antagonists, those containing a 1,2,4-triazolo[1,5-*a*]quinoxaline scaffold have been extensively explored, showing to be an extremely versatile motif during the identification of new valuable and selective AR ligands. To the best of our knowledge, most of the published SAR studies related to this chemotype have been devoted to investigate the effect of different substituents (H, COOR, Aryl, Het.) at position 2[39] and to study the consequences of the bioisosteric replacement on the azole ring[39] (triazole, imidazole) while the introduction of diversity at position 4 remained almost unexplored until recently.[43] In this scenario, and as a part of our interest in the search for novel adenosine receptor antagonists,[47,48] we aimed to evaluate the adenosine antagonistic profile at the human receptors of a series of 4-substituted 2-(2′-furyl)-1,2,4-triazolo[1,5-*a*]quinoxalines (Fig. 2). Further motivation for this work was found in the preliminary result that showed significant affinity differences between human and rat receptors for the parent compound **11** (see Table 3 and Ref. 39). We herein report their synthesis, pharmacological characterisation at the four human adenosine receptors and 3D-QSAR studies for the case of the hA_1 receptor.

1.1. Chemistry

The general method employed for the synthesis of the 4-substituted-2-(2′-furyl)-1,2,4-triazolo[1,5-*a*]quinoxalines **9**–**12** is illustrated in Schemes 1 and 2 and follow the comprehensive procedures described by Cecchy et al.[39] for this heterocyclic system. Scheme 1 describes the synthetic pathway which led to the 1,2,4-triazolo-[1,5-*a*]quinoxaline core, briefly, reaction of 2-nitrophenylhydrazine **1** with the 2-furoic anhydride **2** afford the hydrazide **3** in excellent yield (96%). Deshydrochlorination of **3** was performed at reflux in phosphorus oxychloride for 45 min (70%) (Scheme 1). Treatment of the iminochloride **4** with ammonium hydroxide in a sealed tube yielded the amidine **5** (98%) as a bright red solid which was cyclized to 1,2,4-triazole **6** (92%) by reaction with ethoxyoxalyl chloride. The reflux conditions required to reduce the nitro group in **6**, employing iron in glacial acetic acid, additionally promote ring closure, yielding the tricyclic derivative **7** (98%). Reaction of 2-furyl-1,2,4-triazolo[1,5-*a*]quinoxalin-4-one **7** with phosphoryl oxychloride allows to isolate (80%) the key intermediate **8** (Scheme 1).

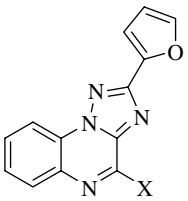

Figure 2. General structure of the obtained 4-substituted 2-(2′-furyl)-1,2,4-triazolo[1,5-*a*]quinoxalines.

The structural diversification performed at the position 4 of the heterocyclic system is shown in Scheme 2. Nucleophilic replacement of the chloro atom at the highly reactive iminochloride **8** by ammonia, amines or alcohols afforded amines **9**, **11** and ethers **10**, respectively (Tables 1 and 2). Finally, the synthesis of the amides **12** has been performed by direct acylation allowing to react **11** with acyl chlorides in pyridine (Scheme 2, Tables 1 and 2). Most relevant analytical and spectroscopic data of obtained compounds are described in Tables 1 and 2.

2. Pharmacology

The binding activities of the obtained compounds at the four human adenosine receptors subtypes were determined using radioligand binding assays procedures (see Section 5). The affinity of those compounds that did not fully displace radioligand binding was expressed as the percentage of inhibition of specific binding at 10^{-6} M (Table 3).

3. Results and discussion

Affinities of 4-substituted 2-(2′-furyl)-1,2,4-triazolo[1,5-*a*]quinoxalines **9**–**12** in radioligand binding assays at

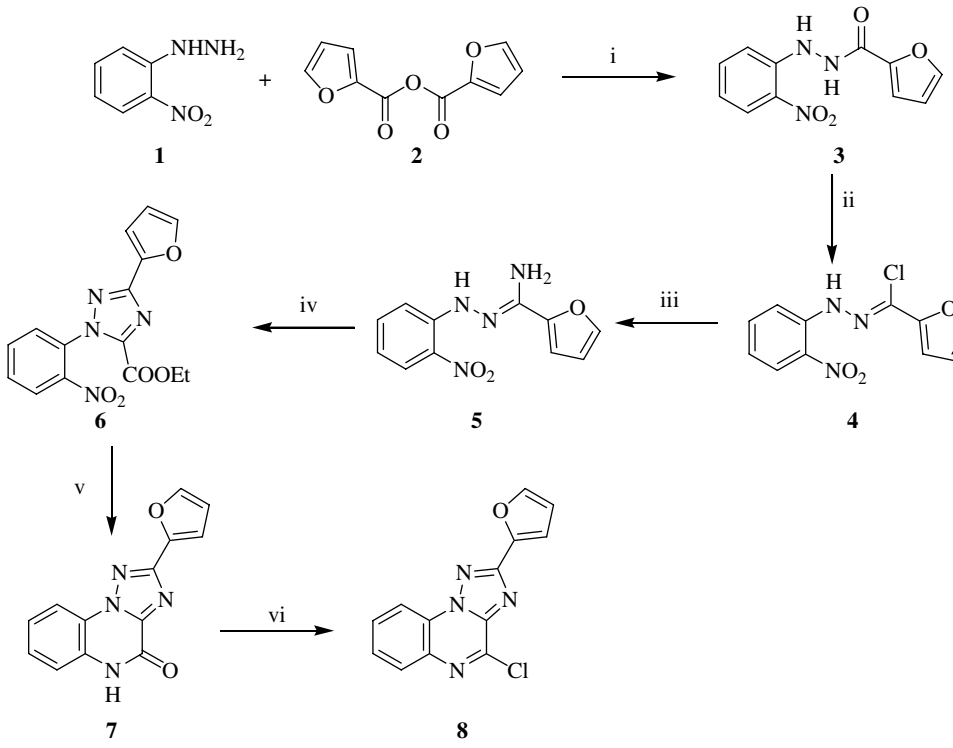

Scheme 1. Synthesis of the 2-(2′-furyl)-1,2,4-triazolo[1,5-*a*]quinoxaline core. Reagents and conditions: (i) EtOH, reflux; (ii) $POCl_3$, reflux; (iii) NH_3/100 °C; (iv) ClCOCOOEt, reflux; (v) Fe/AcOH, reflux; (vi) $POCl_3$.

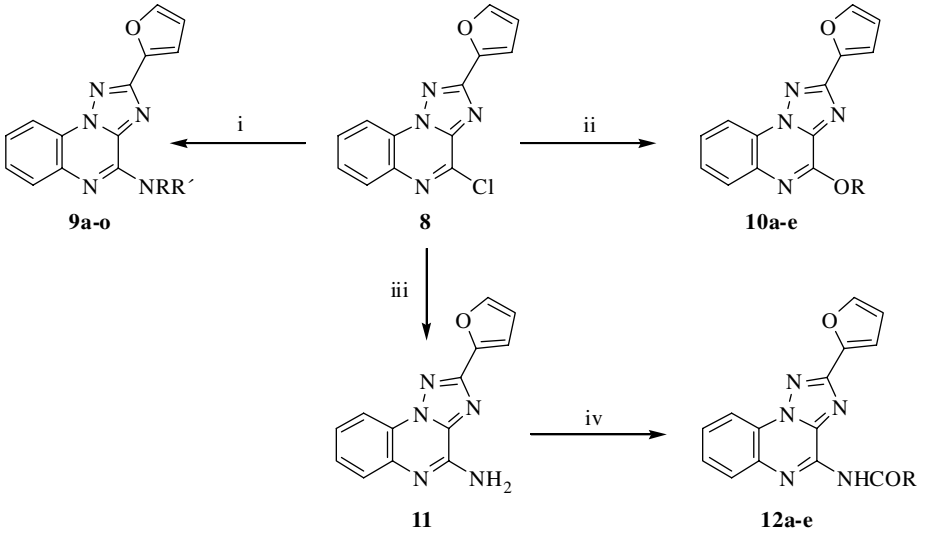

Scheme 2. Synthesis of 4-substituted 2-(2′-furyl)-1,2,4-triazolo[1,5-*a*]quinoxalines. Reagents and conditions: (i) RNHR/EtOH, 100 °C; (ii) ROH/THF, NaH; (iii) NH_3; (iv) RCOCl/pyridine.

the four human adenosine receptors (A_1, A_{2A}, A_{2B} and A_3) are reported in Table 3. It should first be pointed out that, in our hands, the affinity elicited for the early described amine **11** at the human A_1 receptors was slight superior to the values described in the literature[39] ($pK_i = 7.52$ vs $pK_i = 8.25$), most probably due to either the different species of the receptor employed during the studies (rat vs human) or the experimental differences among both assays. Examination of the binding results listed in Table 3 indicated that several potents, but lightly selective, adenosine ligands were identified. Moreover, the obtained data confirmed our initial hypothesis that the structural modifications carried out on the 4-position of the tricyclic system produces a remarkable modification of the adenosine receptorial profile in terms of affinity and/or selectivity.

The 4-amino derivatives (**9a**–**o** and **11**) represent the most populated set of compounds obtained during this study (16 derivatives). As expected, replacement of

Table 1. Structure of the obtained 4-substituted 2-(2′-furyl)-1,2,4-triazolo[1,5-*a*]-quinoxalines **9**–**12**

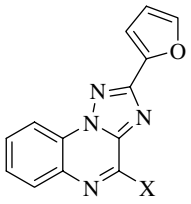

Compound	X	Mp (°C)	Recr. solvent	Yield (%)
11	NH_2	276–277	EtOH	78
9a	NHPh	214–216	MeOH	85
9b	$NHCH_2Ph$	149–151	MeOH	73
9c	$NHCH_2$-(2-Furyl)	177–179	MeOH	82
9d	$NHCH_2CH_2Ph$	241–243	MeOH	88
9e	$NHCH_2CH_2OH$	202–204	MeOH	73
9f	$NHCH_2CH(OH)CH_3$	185–187	*i*-PrOH	73
9g	$NHCH_2CH(OH)CH_2NH_2$	141–143	MeOH	73
9h	$NHCH_2CH_2OCH_3$	113–114	*i*-PrOH	91
9i	$NHCH_2CH_2CH_2OCH_3$	108–110	MeOH	71
9j	$NHCH_2CH(OCH_3)_2$	121–123	*i*-PrOH	82
9k	$N(CH_3)_2$	144–146	*i*-PrOH	91
9l	$N(CH_2CH_3)_2$	105–106	EtOH	69
9m	$N(CH_2CH_2OH)_2$	210–212	MeOH	88
9n	$N(CH_2CH_2)_2NH$	156–157	*i*-PrOH	93
9o	$N(CH_2CH_2)_2N–CH_2CH_2OH$	272–274	MeOH	65
10a	OCH_3	174–176	MeOH	68
10b	OCH_2CH_3	163–165	MeOH	64
10c	OCH_2Ph	206–208	*i*-PrOH	45
10d	OCH_2-(2-Furyl)	191–193	MeOH	80
10e	OCH_2-(3-Furyl)	176–178	*i*-PrOH	73
12a	$NHCOCH_3$	224–226	MeOH	28
12b	$NHCOCH_2Ph$	228–230	*i*-PrOH	18
12c	$NHCOCH_2CH_2Ph$	189–190	*i*-PrOH	44
12d	NHCO-(2-Furyl)	266–267	MeOH	23
12e	NHCO-(2-Thienyl)	234–236	*i*-PrOH	18

hydrogen atoms in the amino group of the parent compound of the series (**11**) to obtain different secondary and tertiary amines had contrasting pharmacological effects on the affinity and selectivity profiles. Thus, phenylation of **11** to give **9a** reduced the affinity towards all adenosine receptor subtypes (Table 3). A similar behaviour is observed for the N-side chain superior homologues of **9a** (**9b** and **9c**). A comparison of the biological data obtained for the 4-benzyl and 4-furfuryl 1,2,4-triazolo[1,5-*a*]quinazolines (**9b** and **9c**) reveals that the substitution of the phenyl ring by the furan produced a moderate (fivefold) increase in potency at the hA_1 receptor and, simultaneously, improve the selectivity towards the other adenosine receptor subtypes. In general, introduction of amines containing a 2-hydroxyethyl fragment (**9e**, **9f**, **9g**, **9m**) positively influences the hA_1 and the hA_3 binding activity, while decreases hA_{2A} and hA_{2B} affinity. It is worth noting that the 2-hydroxyethylamino derivative **9e** possess the highest hA_1AR affinity ($pK_i = 8.50$) among the herein reported compounds. As observed in Table 3 the modifications designed to evaluate the role of the alcoholic function on the lead compound **9e** [e.g., introduction of substituents in the carbon β of the alkyl chain (methyl **9f** or aminomethyl **9g**) and ether formation (**9h**, **9i**, **9j**)] afforded derivatives with attenuated biological activity. These data suggest the importance in the binding site of possible moieties with hydrogen-bond acceptor capabilities. A dramatic drop of affinity was observed for tertiary or heterocyclic amines, (**9k**, **9l**, **9n**, **9o**) a result which confirm the occurrence of a strong interaction of the NHR group at 4 position with a hydrogen-bond acceptor in the active binding site.[46] Interestingly, in this series the most remarkable compound is the bis-2-hydroxyethyl derivative (**9m**) which elicited a moderate hA_1 affinity ($pK_i = 7.23$). Such a result suggests that the lack of the NH group could be partially counterbalanced by the presence of two highly flexible carbinol moieties of the alkyl chain, thus recovering the capacity of hydrogen-bond interaction with the receptor.

Introduction of alcohoxy groups at 4 (**10a**, **10b**, **10c**) produces an important decrease in the antagonistic AR activity (Table 3). The weak hA_3 antagonistic activity observed for the benzyl derivative **10c** aimed us to prepare the furyl analogues **10d** and **10e**. In these pair of compounds, with diminished lipophilicity on the substitution at 4, an increased A_3 binding affinity is observed. Moreover, derivative **10d** showed to be not only

Table 2. Analytical and spectroscopic data of 4-substituted 2-(2′-furyl)-1,2,4-triazolo[1,5-*a*]quinoxalines **9**–**12**

Compound	MS (M^+) *m*/*z* (%)	^{1}H NMR ($CDCl_3$/TMS) δ (ppm), *J* (Hz)	Analysis C, H, N (Calcd/Found)
11	251 (100)	8.29 (d, *J* = 8.1, 1H), 7.78 (d, *J* = 8.0, 1H), 7.70–7.40 (m, 3H), 7.22 (d, *J* = 3.0, 1H), 6.76 (m, 1H), 5.82 (br s, 2H)	C (62.15/62.32), H, (3.61/3.68), N (27.87/27.97)
9a	327 (83)	8.12 (dd, *J* = 8.0, 1.1, 1H), 7.89–7.86 (m, 3H), 7.73 (dd, *J* = 8.1, 1.1, 1H), 7.52 (br s, 1H), 7.39–7.28 (m, 4H), 7.09 (d, *J* = 3.3, 1H), 7.02 (d, *J* = 7.3, 1H), 6.47 (dd, *J* = 3.3, 1.7, 1H)	C (69.71/70.02), H, (4.00/4.12), N (21.39/21.54)
9b	341 (62)	8.25 (dd, *J* = 8.1, 1.1, 1H), 7.79 (d, *J* = 8.0, 1H), 7.60 (d, *J* = 0.7, 1H), 7.51–7.25 (m, 7H), 7.16 (d, *J* = 3.3, 1H), 6.56 (dd, *J* = 3.3, 1.7, 1H), 6.48 (t, *J* = 5.4, 1H), 4.87 (d, *J* = 5.4, 2H)	C (70.37/70.52), H, (4.43/4.65), N (20.52/20.78)
9c	331 (72)	8.25 (dd, *J* = 8.1, 1.3, 1H), 7.79 (dd, *J* = 8.1, 1.3, 1H), 7.61 (dd, *J* = 1.7, 0.6, 1H), 7.53 (m, 3H), 7.17 (dd, *J* = 3.4, 0.6, 1H), 6.57 (dd, *J* = 3.4, 1.7, 1H), 6.42–6.31 (m, 3H), 4.90 (d, *J* = 5.2, 2H)	C (65.25/65.29), H, (3.95/4.10), N (21.14/21.37)
9d	355 (20)	8.26 (dd, *J* = 8.1, 1.1, 1H), 7.80 (dd, *J* = 8.1, 1.1, 1H), 7.62 (d, *J* = 0.9, 1H), 7.52 (m, 1H), 7.47 (d, *J* = 1.3, 1H), 7.37–7.15 (m, 6H), 6.58 (dd, *J* = 3.4, 1.7, 1H), 6.28 (br s, 1H), 4.00 (m, 2H), 3.07 (m, 2H)	C (70.97/71.21), H, (4.82/4.95), N (19.71/19.79)
9e	295 (30)	8.20 (dd, *J* = 8.1, 1.1, 1H), 7.71 (d, *J* = 8.1, 1H), 7.66 (d, *J* = 0.9, 1H), 7.52 (m, 1H), 7.41 (m, 1H), 7.18 (d, *J* = 3.4, 1H), 6.61 (dd, *J* = 3.4, 1.7, 1H), 3.93 (t, *J* = 4.8, 2H), 3.84 (t, *J* = 4.8, 2H)	C (61.01/61.22), H, (4.44/4.61), N (23.72/24.01)
9f	309 (20)	8.21 (dd, *J* = 7.9, 1.0, 1H), 7.68 (d, *J* = 1.1, 1H), 7.60 (d, *J* = 0.9, 1H), 7.48–7.36 (m, 2H), 7.34 (d, *J* = 0.9, 1H), 7.14 (d, *J* = 3.0, 1H), 6.68 (br s, 1H), 6.56 (dd, *J* = 3.3, 1.5, 1H), 4.72 (m, 1H), 4.22 (m, 1H), 3.88 (m, 1H), 3.69 (m, 1H), 1.32 (s, 3H)	C (62.13/62.25), H, (4.89/4.97), N (22.64/22.91)
9g	324 (10)	8.22 (d, *J* = 8.1, 1H), 7.71 (d, *J* = 8.1, 1H), 7.59 (m, 1H), 7.51–7.30 (m, 2H), 7.15 (d, *J* = 3.5, 1H), 6.70 (br s, 1H), 6.55 (d, *J* = 3.5, 1H), 3.93 (m, 2H), 3.74 (m, 1H), 2.91 (m, 2H), 2.72 (br s, 2H)	C (59.25/59.43), H, (4.97/5.08), N (25.91/26.25)
9h	309 (25)	8.21 (d, *J* = 8.0, 1H), 7.71 (d, *J* = 8.0, 1H), 7.60 (m, 1H), 7.42 (m, 1H), 7.34 (m, 1H), 7.16 (d, *J* = 2.8, 1H), 6.55 (d, *J* = 1.3, 1H), 3.88 (m, 2H), 3.68 (m, 2H), 3.40 (s, 3H), 2.30 (br s, 1H)	C (62.13/62.32), H, (4.89/4.99), N (22.64/22.87)
9i	323 (35)	8.22 (d, *J* = 8.1, 1H), 7.74 (d, *J* = 8.1, 1H), 7.62 (m, 1H), 7.60 (t, *J* = 7.6, 1H), 7.35 (t, *J* = 7.6, 1H), 7.18 (d, *J* = 3.3, 1H), 6.58 (m, 1H), 6.40 (m, 1H), 3.80 (m, 2H), 3.49 (t, *J* = 5.9, 2H), 3.39 (s, 3H), 2.04 (m, 2H)	C (63.15/63.32), H, (5.30/5.41), N (21.66/21.85)
9j	339 (10)	8.30 (dd, *J* = 8.0, 1.4, 1H), 7.70 (dd, *J* = 8.0, 1.4, 1H), 7.64 (dd, *J* = 1.5, 0.6, 1H), 7.51–7.40 (m, 2H), 7.21 (dd, *J* = 3.5, 0.6, 1H), 6.58 (dd, *J* = 3.5, 1.5, 1H), 6.20 (br s, 1H), 4.67 (m, 1H) 3.90 (m, 2H), 3.47 (s, 6H)	C (60.17/60.32), H, (5.05/5.11), N (20.64/20.75)
9k	279 (51)	8.22 (dd, *J* = 8.1, 1.1, 1H), 7.68–7.61 (m, 2H), 7.41 (d, *J* = 8.1, 1H), 7.32 (dd, *J* = 3.3, 1.7, 1H), 7.15 (d *J* = 3.3, 1H), 6.56 (d *J* = 1.7, 1H), 3.59 (s, 6H)	C (64.51/64.59), H, (4.69/4.87), N (25.07/25.21)
9l	307 (45)	8.16 (dd, *J* = 8.1, 1.3, 1H), 7.59–7.52 (m, 2H), 7.33 (m, 1H), 7.07 (d, *J* = 3.4, 1H), 6.47 (dd, *J* = 3.4, 1.8, 1H), 4.02 (q, *J* = 7.0, 4H), 1.25 (t, *J* = 7.0, 6H)	C (66.43/66.52), H, (5.58/5.67), N (22.79/23.01)
9m	339 (35)	8.24 (d, *J* = 6.4,1H), 7.62–7.54 (m, 2H), 7.47–7.40 (m, 2H), 7.15 (m, 1H), 6.56 (m, 1H), 4.20 (m, 4H), 4.04 (m, 4H)	C (60.17/60.24), H, (5.05/5.14), N (20.64/20.80)
9n	320 (30)	8.30 (dd, *J* = 8.1, 1.2, 1H), 7.71 (dd, *J* = 8.1, 1.2, 1H), 7.63 (m, 1H), 7.53 (m, 1H), 7.48 (m, 1H), 7.21 (m, 1H), 6.58 (dd, *J* = 3.3, 1.7, 1H), 4.34 (m, 4H), 3.10 (m, 4H), 2.85 (br s, 1H)	C (63.74/63.79), H, (5.03/5.21), N (26.23/26.38)
9o	364 (60)	8.28 (dd, *J* = 8.0, 1.2, 1H), 7.72 (dd, *J* = 8.0, 1.2, 1H), 7.63–7.34 (m, 2H), 7.20 (d, *J* = 3.3, 1H), 6.58 (dd, *J* = 3.3, 1.7, 1H), 4.41 (m, 4H), 3.71 (m, 2H), 2.72 (m, 4H), 2.62 (m, 2H), 2.04 (br s, 1H)	C (62.62/62.72), H, (5.53/5.68), N (23.06/23.17)
10a	266 (100)	8.46 (dd, *J* = 7.7, 1H), 8.39 (m, 1H), 8.10 (d, *J* = 7.7, 1H), 7.60–7.50 (m, 2H), 7.32 (m, 1H) 6.60 (s, 1H), 4.29 (s, 3H)	C (63.15/63.31), H, (3.79/3.97), N (21.04/21.26)
10b	280 (100)	8.40 (m, 1H), 7.90 (m, 1H), 7.65 (dd, *J* = 1.7, 0.9, 1H), 7.61–7.57 (m, 2H), 7.32 (d, *J* = 3.4, 1H), 6.60 (dd, *J* = 3.4, 1.7, 1H), 4.79 (q, *J* = 7.1, 2H), 1.60 (t, *J* = 7.1, 3H)	C (64.28/64.33), H, (4.32/4.45), N (19.99/20.17)
10c	342 (30)	8.35 (1H, m), 7.88 (1H, m), 7.62–7.53 (5H, m), 7.41–7.26 (4H, m), 6.57 (dd, *J* = 3.4, 1.7, 1H), 5.57 (s, 2H)	C (70.17/70.35), H, (4.12/4.22), N (16.37/16.51)
10d	332 (25)	8.40 (m, 1H), 7.94 (m, 1H), 7.63 (m, 3H), 7.45 (dd, *J* = 1.8, 0.7, 1H), 7.30 (dd, *J* = 3.3, 0.7, 1H), 6.62 (d, *J* = 3.3, 1H), 6.58 (dd, *J* = 3.3, 1.8, 1H), 6.38 (dd, *J* = 3.3, 1.8, 1H)	C (65.06/65.22), H, (3.64/3.81), N (16.86/17.01)
12a	293 (20)	8.78 (br s, 1H), 8.38 (m, 1H), 8.02 (m, 1H), 7.68–7.62 (m, 3H), 7.24 (dd, *J* = 3.4, 0.5, 1H), 6.62 (dd, *J* = 3.4, 1.7, 1H), 2.74 (s, 3H)	C (61.43/61.52), H, (3.78/4.00), N (23.88/23.97)

(*continued on next page*)

Table 2 (*continued*)

Compound	MS (M^+) *m/z* (%)	^{1}H NMR ($CDCl_3$/TMS) δ (ppm), *J* (Hz)	Analysis C, H, N (Calcd/Found)
12b	369 (15)	8.85 (br s, 1H), 8.37 (m, 1H), 8.05 (m, 1H), 7.66–7.62 (m, 3H), 7.45–7.26 (m, 6H), 7.20 (dd, *J* = 3.4, 0.6, 1H), 6.60 (dd, *J* = 3.4, 1.8, 1H), 4.37 (s, 2H)	C (68.28/68.41), H, (4.09/4.18), N (18.96/19.02)
12c	383 (52)	8.77 (br s, 1H), 8.37 (m, 1H), 8.00 (m, 1H), 7.65–7.61 (m, 3H), 7.33–7.18 (m, 5H), 6.61 (dd, *J* = 3.5, 1.7, 1H), 3.39 (m, 2H), 3.16 (m, 2H)	C (68.92/69.07), H, (4.47/4.54), N (18.27/18.35)
12d	345 (25)	9.61 (br s, 1H), 8.45 (br s, 1H), 8.24 (m, 1H), 7.71–7.68 (m, 3H), 7.45 (m, 1H), 7.33 (d, *J* = 3.4, 1H), 6.60 (m, 1H)	C (62.61/62.74), H, (3.21/3.40), N (20.28/20.42)
12e	361 (26)	11.60 (br s, 1H), 8.44 (m, 1H), 8.22–7.84 (m, 6H), 7.32 (m, 2H), 6.76 (m, 1H)	C (59.82/60.00), H, (3.07/3.24), N (19.38/19.53)

Table 3. Structure and affinity binding data of the obtained 4-Substituted 2-(2′-furyl)-1,2,4-triazolo[1,5-*a*]-quinoxalines **9**–**12** at the human adenosine receptors

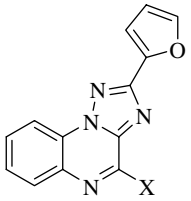

Compound	X	Human adenosine receptors (pK_i or % inhibition at 10^{-6} M)			
		A_1	A_{2A}	A_{2B}	A_3
11	NH_2	8.25 ± 0.12	7.95 ± 0.10	7.88 ± 0.08	6.48 ± 0.07
9a	NHPh	7.34 ± 0.12	7.19 ± 0.06	49 ± 4%	71.7 ± 3%
9b	$NHCH_2Ph$	6.99 ± 0.09	6.52 ± 0.05	24 ± 4%	32.6 ± 4%
9c	$NHCH_2$-(2-Furyl)	7.48 ± 0.20	6.31 ± 0.15	5.76 ± 0.10	57.3 ± 1%
9d	$NHCH_2CH_2Ph$	7.03 ± 0.16	7.29 ± 0.10	46 ± 5%	6.43 ± 0.15
9e	$NHCH_2CH_2OH$	8.50 ± 0.21	7.20 ± 0.13	6.91 ± 0.15	7.52 ± 0.15
9f	$NHCH_2CH(OH)CH_3$	8.40 ± 0.07	7.32 ± 0.10	7.17 ± 0.13	7.64 ± 0.19
9g	$NHCH_2CH(OH)CH_2NH_2$	6.85 ± 0.14	57 ± 4%	34 ± 3%	43 ± 4%
9h	$NHCH_2CH_2OCH_3$	6.52 ± 0.08	5.51 ± 0.10	32 ± 4%	6.36 ± 0.10
9i	$NHCH_2CH_2CH_2OCH_3$	7.13 ± 0.10	6.43 ± 0.18	6.37 ± 0.08	82 ± 3%
9j	$NHCH_2CH(OCH_3)_2$	6.24 ± 0.10	20 ± 2%	22 ± 5%	55.3 ± 4%
9k	$N(CH_3)_2$	31.10 ± 3%	6.51 ± 0.09	17 ± 2%	50.7 ± 3%
9l	$N(CH_2CH_3)_2$	6.87 ± 0.23	6.40 ± 0.08	5.62 ± 0.15	10.4 ± 2%
9m	$N(CH_2CH_2OH)_2$	7.23 ± 0.10	6.96 ± 0.21	46 ± 4%	51.7 ± 2%
9n	$N(CH_2CH_2)_2NH$	12.30 ± 2%	7 ± 2%	4 ± 1%	26.7 ± 3%
9o	$N(CH_2CH_2)_2N$–CH_2CH_2OH	24.54 ± 3%	12 ± 4%	3 ± 2%	24 ± 4%
10a	OCH_3	6.48 ± 0.14	6.4 ± 0.07	28 ± 3%	57.4 ± 2%
10b	OCH_2CH_3	5.43 ± 0.13	38 ± 2%	34 ± 4%	69 ± 1%
10c	OCH_2Ph	13.83 ± 4%	38 ± 3%	3 ± 2%	5.81 ± 0.10
10d	OCH_2-(2-Furyl)	55.11 ± 3%	8 ± 1%	3 ± 2%	7.18 ± 0.07
10e	OCH_2-(3-Furyl)	6.27 ± 0.2	6.24 ± 0.07	6.84 ± 0.1	6.17 ± 0.10
12a	$NHCOCH_3$	6.95 ± 0.12	6.70 ± 0.12	6.6 ± 0.14	6.60 ± 0.06
12b	$NHCOCH_2Ph$	7.2 ± 0.07	6.8 ± 0.10	6.6 ± 0.05	7.0 ± 0.08
12c	$NHCOCH_2CH_2Ph$	7.9 ± 0.20	7.2 ± 0.05	6.3 ± 0.06	6.9 ± 0.12
12d	NHCO-(2-Furyl)	6.7 ± 0.12	6.4 ± 0.02	5.6 ± 0.08	6.6 ± 0.13
12e	NHCO-(2-Thienyl)	7.3 ± 0.06	10 ± 2%	21 ± 3%	52 ± 3%

a relatively potent (pK_i = 7.18) but also a highly selective ligand of the A_3 receptor subtype. The next exploration consisted on the replacement of one of the hydrogen atoms of the amino group at **11** by acyl or aroyl fragments to afford amides **12**. Such an exploration aimed to validate previous findings reported in analogous heteroaromatic systems regarding the modification of the affinity and selectivity profile as a consequence of the increased acidity of the NH moiety.[21,30,48] As observed in Table 3, amidation of the amino group at 4 position of the heteroaromatic system produces no improvements in affinity at any receptor subtype. The only remarkable information extracted from this series is the data obtained for the 2-thienoyl derivative **12e**, which is a relatively potent (pK_i = 7.3) and highly selective hA_1 antagonist.

A 3D-QSAR modelling study was performed by means of the GRIND/ALMOND methodology,[49] in order to gain insight into the structure–activity relationships derived from the variability explored in position 4. Interpretable models need to be constructed using a minimum set of compounds that offers a large enough window of activities. For this reason, only hA_1 ($n = 21$ compounds, $\Delta pK_i = 3.1$ log units) and hA_{2A} models ($n = 18$ compounds, $\Delta pK_i = 2.4$ log units) were attempted. Given the high planarity of the 1,2,4-triazolo[1,5-*a*]-quinoxaline scaffold, the only existing conformational degree of freedom is the bond that links the quinoxaline and furane rings. The torsional angle (N4–C3–C2–O) was explored through a quantum mechanical torsion scan performed on the parent compound **11**. As a result, two local minima were found with the 2-furyl located co-planar with respect to the quinoxaline scaffold, that is, with the oxygen pointing in the same direction of N4 (conformation A) or in the direction of N2 (conformation B). The small energy difference between both conformations (0.9 kcal/mol) justified the construction of two independent QSAR models, considering either A or B conformation. However, this conformational variability had a minimum impact on the performance of the models (see Table 4). Given that the statistical performance is slightly better in the model generated from conformation A in both the A_1 and A_{2A} receptors, we will only discuss about that model from now on.

The 3D-QSAR model for hA_1AR activities had a satisfactory statistical quality, both in terms of fitting and internal validation. Due to its negligible impact on the model, the DRY probe was removed from the initial set of probes. This is reasonable, since only a few molecules presented any favourable region for the interaction with the DRY probe in the area corresponding to the variable region (substituent in 4 of the quinoxaline scaffold). More surprising is the fact that the inclusion of TIP probe,[50] which captures the differences in the shape due to the different substitutions explored in position 4, does not influence the model. This means that the size variability in the present series has little correlation with the activities. Therefore, the most successful and explanatory model was built using only 3 correlograms (O–O, N1–N1 auto-correlograms and O–N1 cross-correlogram) containing a total number of 74 variables, after one FFD selection cycle. The PLS regression considering 3 latent variables (LV) resulted in a statistically satisfactory model ($r^2 = 0.82$, $q^2_{(LOO)} = 0.64$). As stated before, the inclusion of the TIP probe not only complicates the model, but also reduces slightly the predictability (3 LV, $r^2 = 0.85$, $q^2_{(LOO)} = 0.56$). The interpretation of the model is on the same trend as the SAR observations. The presence of an H-bond donor in the variable region (4-substitution) is favourable for the hA_1 activity. This is captured by the regions with highest PLS coefficient, located in the O–N1 cross-correlogram, depicting a pharmacophoric distance of 10 Å between H-bond donor in position 4 and the H-bond acceptor region corresponding to N2 in the heterocycle (Fig. 3A). Interestingly, the only molecule not bearing a NH-R substituent that shows high values for these variables is the active compound **9m**, which has a tertiary amine with two free hydroxyl groups. The presence of two H-bond donors (e.g., compounds **9e**, **9f**, **9m** and **11**) strengths for hA_1 activity.

To further investigate the shape tolerance of the hA_1 binding site, the 5 molecules without K_i values were included in a QSAR model for *qualitative* predictions.[51] This was done using the technique of PLS combined with a discriminant analysis (PLS-DA), by transforming the activity values in discrete binary values: 0 if $pK_i < 6.5$ or absence of pK_i, 1 for $pK_i > 5$. This cutoff was selected to equilibrate the number of actives and inactives, but after a first inspection compound 9l ($pK_i = 6.87$) was identified as an outlier and left out for further consideration, resulting in a final set of 15 actives and 10 inactives. Once more, we found that the best

Table 4. Statistics of PLS models for the A_1 and A_{2A} human adenosine receptors

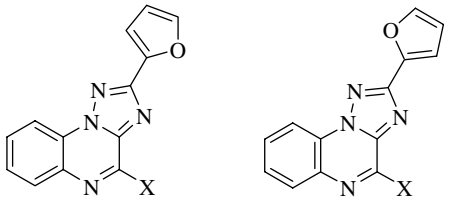

A B

Receptor	*n*	Conformation	LV	r^2	q^2	SDEC	SDEP
hA_1AR	21[a]	A	3	0.82	0.64	0.31	0.44
		B	3	0.82	0.60	0.31	0.46
	25[b]	A	2	0.98	0.89	0.27	0.39
$hA_{2A}AR$	18[a]	A	3	0.92	0.70	0.15	0.30
		B	2	0.88	0.62	0.19	0.33

All the models were built with single FFD run and LOO standard validation procedure.
[a] Only compounds with experimentally available pK_i were included in the models.
[b] PLS-DA model. Compound **9l** was left out as an outlier.

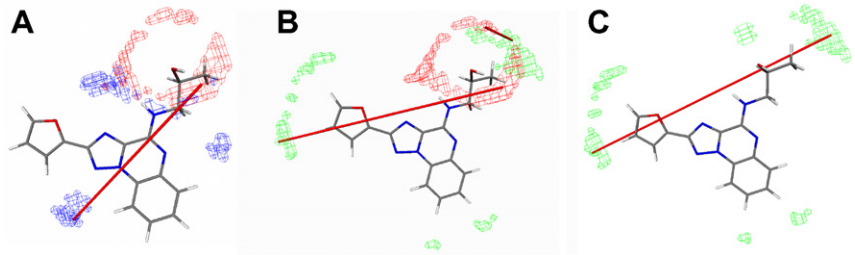

Figure 3. Active compound **9f** is represented with the corresponding MIFs used to generate the 3D-QSAR models. The most relevant GRIND descriptors (with high PLS coefficients) are represented by a red bar. (A) Most important distance between H-bond donor (red) and H-bond acceptor (blue) regions for the hA_1 model. The same region also has high relevance for the A_{2A} model. (B) The most relevant descriptors for the O-TIP cross-correlogram in the hA_{2A} model. (C) Molecular shape, showing the optimum distance between the 2-furlyl substitution and the variable substituent in position 4 as observed in the hA_{2A} model.

model (2 LV, $r^2 = 0.98$, $q^2 = 0.89$) was obtained by only taking into consideration the N1 and O MIFs, thus confirming that the present series do not explore the limits of the shape or flexibility of the binding site of the hA_1 receptor. The interpretability of the model is analogous to what is described above for the model developed for *qualitative* predictions. It is worth to note the excellent statistical parameters of this model, showing a clear capacity to distinguish between active and inactive compounds using the aforementioned description of the molecules.

Regarding the A_{2A} receptor, the statistical quality of a 3D-QSAR model that only considers the O and N1 probes has unacceptable statistical parameters (3LV, $r^2 = 0.83$, $q^2_{(LOO)} = 0.35$) while the inclusion of the shape probe (TIP) significantly improves these values (3LV, $r^2 = 0.92$, $q^2_{(LOO)} = 0.70$). Therefore, as opposed to the hA_1 receptor, the consideration of the molecular shape is determinant for the predictability of a hA_{2A} model. The observation that the highest activity is obtained with a H-bond donor in position 4, with some spatial constrain, is also true for the present case. Thus, highest PLS pseudocoefficients for the O–N1 cross-correlogram establish the same pharmacophoric distance for the H-bond donor in 4 and the H-bond acceptor corresponding to N2 (Fig. 3A). Additionally, in the A_{2A} model the position of this H-bond donor is conditioned by the shape due to the variable region in 4 and the furyl at position 2 of the quinoxaline (Fig. 3B). Finally, the highest PLS coefficient for the TIP auto-correlogram identifies the optimal shape for the most active molecules (TIP–TIP 18 Å, shown in Fig. 3C), which can be related to the depth of the binding pocket of the A_{2A} receptor.

4. Conclusions

In summary, the biological data shown in Table 2 confirm several previous theoretical and experimental studies regarding the importance of the presence of a NH group at position 4 of the heterocyclic system for their interaction with the active binding site in the receptor. Further, our results point that the binding site allocating the explored position of the heterocycle tolerates well substituents with different sterical properties, as exemplified with the observation that even the parent compound **11** (R = H) or compounds bearing relatively bulky substitutions (e.g., **9f**, **11c**) all display good hA_1 affinities. The results of this study clearly reveal that the structural manipulation at position 4 and specially the derivatization of the amino group could allow the discovery of new potent and selective ligands for the hA_1 and hA_3 receptors.

The 3D-QSAR modelling confirmed that the optimum substitution in position 4 should include H-bond acceptor/donor capabilities. The moderate affinity of molecule **9m**, where the lack of NH– in position 4 is counterbalanced with the presence of hydroxyl groups in the variable region, suggests for the presence of a flexible hydrogen-bonding counterpart of position 4 in the hA_1 receptor. This interpretation is reinforced by the fact that the inclusion of TIP probe, which has proven as a very useful tool to correlate the shape of the molecules with their activities,[50–52] had a negligible effect in the hA_1 QSAR model, observed in both the PLS and PLS-DA models. On the contrary, the inclusion of such a description of the molecular shape is essential in order to obtain a predictable model for the hA_{2A} receptor. We can conclude that the binding site of the hA_1 receptor tolerates well the variations within the shape limits explored by the present series, while the hA_{2A} receptor is more restrictive. Whether this is due to a flexible binding pocket in the hA_1 receptor or to a pocket size in this receptor which is greater or equal to the maximum size explored by the present series cannot be determined with the present methodology. All together, the results here reported should guide further chemical explorations of the position 4 of the heterocycle and receptor-based molecular modelling exercises.

5. Experimental

5.1. Synthesis

Melting points were measured on a Gallenkamp apparatus and are uncorrected. Infrared spectra were recorded on a Perkin-Elmer 1640 FT-IR spectrophotometer. ^{1}H NMR spectra were obtained on Bruker WM250 and AM300 spectrometers using tetramethylsilane as internal standard (chemical shifts are δ values, J in Hz). Mass spectra were determined on a Varian MAT-711 instru-

ment. Elemental analyses were performed on a Perkin-Elmer 240B apparatus at the Microanalysis Service of the University of Santiago de Compostela and the obtained results for C, N and H were within ±0.4% of the theoretical values. The progress of the reactions was monitored by thin layer chromatography with 2.5 mm Merck silica gel GF 254 strips, and the purified compounds each showed a single spot; unless otherwise stated iodine vapour and/or UV light were used for detection. Chromatographic separations were performed on silica gel columns by flash chromatography (Kieselgel 40, 0.040–0.063 mm). The synthesis of the precursors **8** and **11** has been performed following the previously described procedure.[36,38,39]

5.2. General procedure for the preparation of amines (9 and 11)

A solution of 4-chloro-2-(2′-furyl)-1,2,4-triazolo[1,5-*a*]quinoxaline **8** (1.1 mmol) in ethanol (8 mL) was mixed with the appropriate amine (2.4 mmol) and potassium iodide (0.020 g) in a sealed tube under argon atmosphere. The reaction mixture was then stirred and heated at 100 °C (oil bath) until the starting material had disappeared (1.5–16 h). After cooling, the solution was concentrated to dryness under reduced pressure and the residue was purified by column chromatography on silica gel to give the corresponding amines **9** and **11**. Further purification was performed by recrystallization of the proper solvent (Tables 1 and 3).

5.3. General procedure for the preparation of ethers (10a–d)

To a solution of 4-chloro-2-(2′-furyl)-1,2,4-triazolo[1,5-*a*]quinoxaline **8** (0.30 mmol) in 4 mL of dry tetrahydrofurane under argon atmosphere were added the appropriate alcohol (0.90 mmol) and sodium hydride (0.90 mmol). The reaction mixture was stirred at room temperature until the starting material had disappeared. (0.5–1 h) and then treated with 5 mL of methanol and 1 mL of water. The solution was concentrated to dryness under reduced pressure and the residue was purified by column chromatography on silica gel to obtain the expected ethers **10**. Further purification was performed by recrystallization of the proper solvent (Tables 1 and 3).

5.4. General procedure for the preparation of amides (12a–e)

To a solution of 4-amino-2-(2′-furyl)-1,2,4-triazolo[1,5-*a*]quinoxaline **11** (0.40 mmol) in 5 mL of dry pyridine under argon atmosphere was added slowly the appropriate acyl chloride (0.80 mmol). The reaction mixture was stirred at room temperature during 8 h and then heated at 40 °C until the starting material had disappeared. (1–6 h). The reaction mixture was then treated with 10% hydrochloric acid and extracted with methylene chloride. The organic extracts were dried (Na_2SO_4), concentrated to dryness under reduced pressure and the residue was purified by column chromatography on silica gel to obtain the expected amides **12**. Further purification was performed by recrystallization of the proper solvent (Tables 1 and 3).

5.5. Pharmacology: radioligands binding studies

Radioligand binding competition assays were performed in vitro as previously described[53] using A_1, A_{2A}, A_{2B} and A_3 human receptors expressed in transfected CHO (A_1), HeLa (A_{2A} and A_3) and HEK-293 (A_{2B}) cells. The experimental conditions used are summarized in Table 5.

In each instance aliquots of membranes (15 μg for A_1, 10 μg for A_{2A}, 18 μg for A_{2B} and 90 μg for A_3) in buffer A (see Table 5) were incubated for the specified period at 25 °C with the radioligand (2–35 nM) and 6 different concentrations (ranging from 0.1 nM to 1 μM) of the test molecule in a final volume of 200 μl. The binding reaction was stopped by rapid filtration in a multiscreen manifold system (Milipore Ibérica, Madrid, Spain). Unbound radioligand was removed by washing four times with 250 μl ice-cold buffer B for A_1 and A_{2A} receptors, and six times 250 μl ice-cold buffer B for A_{2B} and A_3 receptors (see Table 4). Non-specific binding was determined using a 50 or 400 μM NECA solution for A_{2A} and A_{2B} receptors and 10 or 100 μM R-PIA solution for A_1 and A_3, respectively. Radioactivity retained on filters was determined by liquid scintillation counting using Universol (ICN Biochemicals, Inc.). The binding affinities were determined using [^{3}H]DPCPX (130 Ci/mmol; Amersham Biosciences, Barcelona, Spain) as

Table 5. Conditions used for radioligand binding assays using A_1, A_{2A}, A_{2B} and A_3 human receptors

	A_1	A_{2A}	A_{2B}	A_3
Buffer A	20 mM Hepes, 100 mM NaCl, 10 mM $MgCl_2$, 2 U/mL adenosine deaminase (pH 7.4)	50 mM Tris–HCl, 1 mM EDTA, 10 mM $MgCl_2$, 2 U/mL adenosine deaminase (pH 7.4)	50 mM Tris–HCl, 1 mM EDTA, 10 mM $MgCl_2$, 0.1 mM benzamidine, 2 U/mL adenosine deaminase (pH 6.5)	50 mM Tris–HCl, 1 mM EDTA, 5 mM $MgCl_2$, 2 U/mL adenosine deaminase (pH 7.4)
Buffer B	20 mM Hepes, 100 mM NaCl, 10 mM $MgCl_2$, (pH 7.4)	50 mM Tris–HCl, 1 mM EDTA, 10 mM $MgCl_2$ (pH 7.4)	50 mM Tris–HCl (pH 6.5)	50 mM Tris–HCl (pH 7.4)
Plate	GF/C	GF/C	GF/B	GF/B
Radioligand	[^{3}H]DPCPX 2 nM	[^{3}H]ZM241385 3 nM	[^{3}H]DPCPX 35 nM	[^{3}H]NECA 30 nM
Non-specific binding	10 μM (R)-PIA	50 μM NECA	400 μM NECA	100 μM (R)-PIA
Incubation	25 °C/60 min	25 °C/30 min	25 °C/30 min	25 °C/180 min

the radioligand for A_1 and A_{2B}, [^{3}H]ZM241385 (21 Ci/mmol; Tocris, Madrid, Spain) for A_{2A} and [^{3}H]NECA (15.3 Ci/mmol; NEN-Perkin-Elmer Life Sciences, Madrid, Spain) for A_3. The inhibition constant (K_i) of each compound was calculated by the expression: $K_i = IC_{50}/(1 + (C/K_D))$; where IC_{50} is the concentration of compound that displaces the binding of radioligand by 50%, C is the free concentration of radioligand and K_D is the apparent dissociation constant of each radioligand. The percentage of displacement of specific binding was calculated by the expression: % of displacement = ((BT − dpm) * 100)/(BT − NSB); where BT is the total binding of the radioligand in the assay, NSB is the non-specific binding of the radioligand in the assay and dpm are the radioactive measure obtained by competing the radioligand binding with a given concentration of the test compound.

5.6. Molecular modelling

All calculations were run on an AMD-X2 processor running linux (FC 5) operative system. All the GRid independent descriptors (GRIND)[49] of this study were computed and analyzed with the program Almond 3.3.0.[54] This procedure for 3D-QSAR studies consists on three steps. First, a set of molecular interaction fields (MIFs) are computed on the basis of the Grid force field,[55] using selected chemical probes that account for the receptor chemical groups. Then, a selection of the most relevant ligand-probe interaction nodes is done and the resulting filtered nodes are encoded via a MACC2 transform into a set of GRIND variables. These alignment independent descriptors represent geometrical relationships between pairs of the selected MIF nodes, which are usually represented with the so-called 'correlograms', where the product of the interaction energy is plotted against the euclidean distance for a given pair of nodes. The correlogram is composed from 'auto-correlograms' (i.e., the node pairs belong to one MIF) and 'cross-correlograms' (i.e., the node pairs belong to two different MIFs). Additional advantage of the method is that the points in the correlogram can be decoded back into the original MIF descriptors, thus allowing analysis and interpretation of the correlogram in terms of molecular interaction capabilities.

The 3D structures needed for the GRIND computations were automatically generated with the program CORINA[56] from the 2D SDfile of the molecules. Given that the present series share a common rigid structure with only one point of diversity (i.e., substituent in position 4), the conformations obtained from CORINA were used directly for the calculation of the descriptors. To account for the most probable conformation of the 2-furyl ring, a torsion scan for the bond connecting the triazol and furane rings was performed with GAUSSIAN98[57] (keywords HF/6-31G* SCAN). Different combinations of the GRID probes O, N1 and DRY and the recently reported TIP probe[50] were initially considered in different calculations, although not all the probes were considered in the final models (see Section 3). Most of the Almond parameters were set to default values, for example, the ALMD directive was equal to 1, the grid spacing was equal to 0.5 Å, the smoothing window of the correlograms was set to 0.8, and the size of the correlograms was automatically established by the program. The optimum number of nodes and weight of the field was set empirically to 80 nodes and 35% weight. These numbers deviate from the default values of 100 nodes and 50% weight, which is due to the relatively small size of the molecules. A soft variable selection method consisting on one fractional factorial design (FFD) was also applied in all models. Chemometric analyses were performed with the tools included in Almond 3.3 for principal component analysis, PCA,[58] and partial least squares regression, PLS.[59] The optimal number of latent variables (LV) for the PLS regression analyses was selected based on cross-validation procedure (standard leave one our method, LOO).

Acknowledgment

Financial support from Almirall Laboratories (Barcelona) is gratefully acknowledged.

References and notes

1. Von Lubitz, D. K. J. E.; Jacobson, K. A. Behavioral Effects of Adenosine Receptors Stimulation. In *Adenosine and Adenine Nucleotides: From Molecular Biology to Integrative Physiology*; Bellardinelli, L., Pelleg, A., Eds.; Kluwer: Norwell, 1995; pp 489–498.
2. Ralevic, V.; Burnstock, G. *Pharmacol. Rev.* **1998**, *50*, 413.
3. Hess, S. *Expert Opin. Ther. Pat.* **2001**, *11*, 1533.
4. Fredholm, B. B.; Arslan, G.; Haldner, L.; Kull, G.; Schulte, G.; Wasserman, W.; Nauyn-Schmied, A. *Arch. Pharmacol.* **2000**, *362*, 364.
5. Fredholm, B. B.; Ijzerman, A. P.; Jacobson, K. A.; Klotz, K. N.; Linden, J. *Pharm. Rev.* **2001**, *53*, 527.
6. Baraldi, P. G.; Cacciari, B.; Romagnoli, R.; Spalluto, G. *Expert Opin. Ther. Pat.* **1999**, *9*, 515.
7. Muller, C. E. *Curr. Top. Med. Chem.* **2003**, *3*, 445.
8. Muller, C. E. *Curr. Med. Chem.* **2000**, *7*, 1269.
9. Merighi, S.; Mirandola, P.; Varani, K.; Gessi, S.; Leung, E.; Baraldi, P. G.; Tabrizi, M. A.; Borea, P. A. *Pharmacol. Ther.* **2003**, *100*, 31.
10. Baraldi, P. G.; Borea, P. A. *Trends Pharmacol. Sci.* **2000**, *21*, 456.
11. Baraldi, P. G.; Cacciari, B.; Romagnoli, R.; Meringhi, S.; Verani, K.; Borea, P. A.; Spalluto, P. *Med. Res. Rev.* **2000**, *20*, 103.
12. Baraldi, P. G.; Bovero, A.; Fruttarolo, F.; Romagnoli, R.; Tabrizi, M.; Aghazadeh, P.; Delia, V.; Katia, B.; Borea, P. A.; Moorman, A. R. *Bioorg. Med. Chem.* **2003**, *11*, 4161.
13. Beukers, M. W.; Chang, L. C. W.; von Kuenzel, J. K.; Mulder-Krieger, Th.; Spanjersberg, R. F.; Brussee, J.; IJzerman, A. P. *J. Med. Chem.* **2004**, *47*, 3707.
14. Harada, H.; Asano, O.; Hoshino, Y.; Yoshikawa, S.; Matsukura, M.; Kabasawa, Y.; Niijima, J.; Kotake, Y.; Watanabe, N.; Kawata, T.; Inoue, T.; Horizoe, T.; Yasuda, N.; Minami, H.; Nagata, K.; Murakami, M.; Nagaoka, J.; Kobayashi, S.; Tanaka, I.; Abe, S. *J. Med. Chem.* **2001**, *44*, 170.
15. Ozola, V.; Thorand, M.; Diekmann, M.; Qurishi, R.; Schumacher, B.; Jacobson, K. A.; Muller, C. E. *Bioorg. Med. Chem.* **2003**, *11*, 347.

16. Sato, H.; Nagashima, K.; Nomura, H.; Karasawa, A.; Nishikawa, S. *J. Toxicol. Path.* **1999**, *12*, 21.
17. Kozo, Y.; Hideaki, K.; Kiyoshi, S.; Akira, K. *Jpn. J. Pharmacol.* **1994**, *65*, 167.
18. Hideaki, M.; Akira, K.; Kazuhiro, K. *J. Pharmacol. Exp. Ther.* **1993**, *266*, 200.
19. Ochi, M.; Shiozaki, S.; Kase, H. *Neuroscience* **2004**, *127*, 223.
20. Kim, J. S.; Sohn, Y. H. *Adv. Behav. Biol.* **2002**, *51*, 365.
21. Jacobson, K. A.; Ijzerman, A. P.; Linden, J. *Drug Dev. Res.* **1999**, *47*, 45.
22. Fozard, J. R. *Curr. Opin. Pharmacol.* **2003**, *3*, 264.
23. Feostikov, I.; Baggioni, I. *Pharmacol. Rev.* **1997**, *49*, 381.
24. Martinez-Tica, J. F.; Zornow, M. H. *Brain Res.* **2000**, *872*, 110.
25. Di Napoli, P.; Contegiacomo, G.; Taccardi, A. A.; Maggi, A.; Di Muzio, M.; Statile, D.; Giuliani, P.; Di Iorio, P.; Barsotti, A. *J. Clin. Basic Cardiol.* **1999**, *2*, 99.
26. Hamilton, H. W.; Ortwine, D. F.; Worth, D. F.; Badger, E. W.; Bristol, J. A.; Bruns, R. F.; Haleen, S. J.; Steffen, R. P. *J. Med. Chem.* **1985**, *28*, 1071.
27. Doichinova, I. A.; Natcheva, R. N.; Mihailova, D. N. *Eur. J. Med. Chem.* **1994**, *29*, 133.
28. Hayallah, A. M.; Sandoval-Ramírez, J.; Reith, U.; Schobert, U.; Preiss, B.; Schumacher, B.; Daly, J. W.; Müller, C. E. *J. Med. Chem.* **2002**, *45*, 1500.
29. Baraldi, P. G.; Tabrizi, M. A.; Preti, D.; Bovero, A.; Romagnoli, R.; Fruttarolo, F.; Zaid, N. A.; Moorman, A. R.; Varani, K.; Gessi, S.; Merighi, S.; Borea, P. A. *J. Med. Chem.* **2004**, *47*, 1434.
30. Kim, S. A.; Marshall, M. A.; Melman, N.; Kim, H. S.; Müller, C. E.; Linden, J.; Jacobson, K. A. *J. Med. Chem.* **2002**, *45*, 2131.
31. Pastorin, G.; Das Ros, T.; Spatullo, G.; Deflorian, F.; Moro, S.; Cacciari, B.; Saraldi, P. G.; Gessi, S.; Varani, K.; Borea, P. A. *J. Med. Chem.* **2003**, *46*, 4278.
32. Maconi, A.; Pastorin, G.; Da Ros, T.; Spatullo, G.; Gao, Z. G.; Jacobson, K. A.; Baraldi, P. G.; Varani, K.; Moro, S.; Borea, P. A. *J. Med. Chem.* **2002**, *45*, 3579.
33. Colotta, V.; Catarzi, D.; Varano, F.; Cecchi, L.; Filacchioni, G.; Martini, C. *Arch. Pharm. Pharm. Med. Chem.* **1999**, *332*, 39.
34. Muller, C. E.; Dieckman, M.; Thorand, M.; Ozola, V. *Bioorg. Med. Chem. Lett.* **2002**, *12*, 501.
35. Bertelli, L.; Biagi, G.; Giorgi, I.; Manera, C.; Livi, O.; Scartoni, V.; Betti, L.; Giannaccini, G.; Trincavelli, L.; Barili, P. L. *Eur. J. Med. Chem.* **1998**, *33*, 113.
36. Colotta, V.; Cecchi, L.; Catarzi, D.; Conti, G.; Filacchioni, G. *Farmaco* **1993**, *48*, 1051.
37. Calotta, V.; Catarzi, D.; Varano, F.; Cecchi, L.; Filacchioni, G.; Galli, A.; Costagli, C. *Arch. Pharm.* **1997**, *330*, 387.
38. Catarzi, D.; Cecchi, L.; Colotta, V.; Melani, F.; Filacchioni, G. *Farmaco* **1993**, *48*, 1065.
39. Colotta, V.; Cecchi, L.; Filacchioni, G.; Martini, C.; Tacchi, P.; Lucacchini, A. *Eur. J. Med. Chem.* **1995**, *30*, 133.
40. Colotta, V.; Catarzi, D.; Varano, F.; Cecchi, L.; Filacchioni, G.; Martini, C.; Trincavelli, L.; Lucacchini, A. *J. Med. Chem.* **2000**, *43*, 1158.
41. Catarzi, D.; Cecchi, L.; Colotta, V.; Filacchioni, G.; Martini, C.; Tacchi, P. *J. Med. Chem.* **1995**, *38*, 1330.
42. Colotta, V.; Catarzi, D.; Varano, F.; Cechi, L.; Filacchioni, G.; Martini, C.; Trincavelli, L.; Lucacchini, A. *J. Med. Chem.* **2000**, *43*, 3118.
43. Catarzi, D.; Colotta, V.; Varano, C.; Filacchioni, G.; Martini, C.; Trincavelli, L.; Lucacchini, A. *Farmaco* **2004**, *59*, 71.
44. Colotta, V.; Catarzi, D.; Varano, C.; Romana, F.; Lenzi, O.; Filacchioni, G.; Trincavelli, L.; Martini, C.; Trincavelli, F.; Deflorian, F.; Moro, S. *J. Med. Chem.* **2004**, *47*, 3580.
45. Catarzi, D.; Colotta, V.; Varano, C.; Lenzi, O.; Filacchioni, G.; Trincavelli, L.; Martini, C.; Montopoli, C.; Moro, S. *J. Med. Chem.* **2005**, *48*, 7932.
46. Lenzi, O.; Colotta, V.; Catarzi, D.; Varano, C.; Filacchioni, G.; Martini, C.; Trincavelli, L.; Ciampi, O.; Varani, K.; Marighetti, F.; Morizzo, E.; Moro, S. *J. Med. Chem.* **2006**, *49*, 3916.
47. Carotti, A.; Stefanacchi, A.; Raviña, E.; Sotelo, E.; Loza, M. I.; Cadavid, M. I.; Centeno, N. B.; Nicolotti, O. *Eur. J. Med. Chem.* **2004**, *39*, 879.
48. Carotti, A.; Cadavid, M. I.; Centeno, N. B.; Esteve, C.; Loza, M. I.; Martínez, A.; Nieto, R.; Raviña, E.; Sanz, F.; Segarra, V.; Sotelo, E.; Stefanacchi, A.; Vidal, B. *J. Med. Chem.* **2006**, *49*, 282.
49. Pastor, M.; Cruciani, G.; McLay, I.; Pickett, S.; Clementi, S. *J. Med. Chem.* **2000**, *43*, 3233.
50. Fontaine, F.; Pastor, M.; Sanz, F. *J. Med. Chem.* **2004**, *47*, 2805.
51. Afzelius, L.; Masimirembwa, C. M.; Karlen, A.; Andersson, T. B.; Zamora, I. *J. Comput. Aided Mol. Des.* **2002**, *16*, 443.
52. Carosati, E.; Lemoine, H.; Spogli, R.; Grittner, D.; Mannhold, R.; Tabarrini, O.; Sabatini, S.; Cecchetti, V. *Bioorg. Med. Chem.* **2005**, *13*, 5581.
53. Bosch, M. P.; Campos, F.; Niubo, I.; Rosell, G.; Diaz, J. L.; Brea, J.; Loza, M. I.; Guerrero, A. *J. Med. Chem.* **2004**, *47*, 4041.
54. Cruciani, G., Fontaine, F., Pastor, M. Almond 3.3.0. Molecular Discovery, Ltd: Perugia, Italy.
55. Goodford, P. J. *J. Med. Chem.* **1985**, *28*, 849.
56. Gasteiger, J. C.; Rudolph, C.; Sadowski, J. *Tetrahedron Comp. Method* **1990**, *3*, 537.
57. Frisch, M. J.; Trucks, G. W.; Schlegel, H. B.; Scuseria, G. E.; Robb, M. A.; Cheeseman, J. R.; Zakrzewski, V. G.; Montgomery, Jr., J. A.; Stratmann, R. E.; Burant, J. C.; Dapprich, S.; Millam, J. M.; Daniels, A. D.; Kudin, K. N.; Strain, M. C.; Farkas, O.; Tomasi, J.; Barone, V.; Cossi, M.; Cammi, R.; Mennucci, B.; Pomelli, C.; Adamo, C.; Clifford, S.; Ochterski, J.; Petersson, G. A.; Ayala, P. Y.; Cui, Q.; Morokuma, K.; Malick, D. K.; Rabuck, A. D.; Raghavachari, K.; Foresman, J. B.; Cioslowski, J.; Ortiz, J. V.; Baboul, A. G.; Stefanov, B. B.; Liu, G.; Liashenko, A.; Piskorz, P.; Komaromi, I.; Gomperts, R.; Martin, R. L.; Fox, D. J.; Keith, T.; Al-Laham, M. A.; Peng, C. Y.; Nanayakkara, A.; Gonzalez, C.; Challacombe, M.; Gill, P. M. W.; Johnson, B.; Chen, W.; Wong, M. W.; Andres, J. L.; Gonzalez, C.; Head-Gordon, M.; Replogle, E. S.; Pople, J.A. Gaussian 98, Revision A.7, Gaussian: Pittsburgh PA, 1998.
58. Carey, R. N.; Wold, S.; Westgard, J. O. *Anal. Chem.* **1975**, *47*, 1824.
59. Hoskuldsson, A. *J. Chemom.* **1988**, *2*, 211.